Food Hydrocolloids 136 (2023) 108315

Contents lists available at ScienceDirect

Food Hydrocolloids

journal homepage: www.elsevier.com/locate/foodhyd

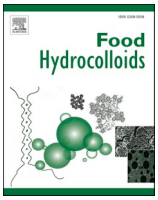

Protein nanofibrils from mung bean: The effect of pH on morphology and the ability to form and stabilise foams

Anja Herneke [a,*], Saeid Karkehabadi [a], Jing Lu [a], Christofer Lendel [b], Maud Langton [a]

[a] Department of Molecular Sciences, Swedish University of Agricultural Sciences (SLU), 750 00, Uppsala, Sweden
[b] Department of Chemistry, Royal Institute of Technology (KTH), 100 40, Stockholm, Sweden

ARTICLE INFO

Keywords:
Plant protein
Foam capacity
Foam stability
Vicilin
8S
Amyloid

ABSTRACT

Protein nanofibrils (PNFs) have potential food uses due to their favorable mechanical and rheological properties. In order to use plant-based protein nanofibrils (PNFs) in new sustainable food applications, a better understanding is needed of the impact of pH on PNFs and their functional properties. In this study, we developed an improved method for generating PNFs from mung bean protein isolate and its globular 8S fraction. We then investigated how these PNFs are affected by increased pH and how pH affects their ability to form stable foams. PNFs were generated in acidic conditions (pH 2) by heating at 85 °C for 2–48 h. Formation of PNFs and the effect of increased pH on their stability were evaluated using thioflavin T fluorescence, electrophoretic gel separation, circular dichroism spectroscopy, atomic force microscopy and viscosity profiling. Foams were made by intense mixing with a homogeniser and evaluated for foam capacity, foam stability and bubble size distribution, using confocal imaging. The results showed that it is possible to optimise the fibrillation conditions for mung bean by generating a more pure initial protein isolate by salt extraction. The results also showed that pH alters the structure of PNFs by degradation and aggregation around the isoelectric point of the protein isolate. At neutral pH, the PNFs were slightly shorter than at the starting pH, but no longer formed aggregates. Fibrillated mung bean protein at pH 4–8 was found to have good foaming properties compared with non-fibrillated protein at the same conditions. The new knowledge generated in this study about how pH alters the structure and foaming properties of PNFs can pave the way for use of PNFs in new innovative food applications.

1. Introduction

With a growing world population and limitations in food supplies, there is rising awareness of the need to change from eating animal-based protein to plant-based protein (Willett et al., 2019). This requires knowledge of how to process plant proteins into new types of materials with specific mechanical properties. Modification by introducing air bubbles is a well-known method for changing the properties of food products, such as texture, appearance and mouthfeel (Murray, 2020). The foaming properties of proteins depend on their ability to form interfacial films to encapsulate the bubbles. Flexible and hydrophilic protein molecules are better foam stabilisers than more rigid molecules, due to their ability to decrease surface tension (Lam, Velikov, & Velev, 2014). Protein is commonly used in the food industry to stabilise foams and there is increasing interest among researchers in using protein aggregates to stabilise the liquid interface in order to create novel food textures (Amagliani & Schmitt, 2017). Transforming proteins into amyloid-like protein nanofibrils (PNFs) can improve the foaming properties compared with the unmodified protein, as demonstrated for PNFs made from β-lactoglobulin (Oboroceanu, Wang, Magner, & Auty, 2014; Peng, Yang, Li, Tang, & Li, 2017) and soybean protein (Wan, Yang, & Sagis, 2016).

Use of food-related PNFs to make new sustainable food applications with attractive functional properties and tailored textures is an emerging research area (Cao & Mezzenga, 2019). PNFs can be generated under different sets of conditions, but one common method involves exposing the protein to an acidic environment and heat treatment. Under these conditions, the proteins are hydrolysed and reassembled into β-sheet rich, nano-sized fibril structures (Sipe et al., 2016). Researchers within material science have long been interested in PNFs, due to the good mechanical and rheological attributes (Ye, Lendel, Langton, Olsson, & Hedenqvist, 2019). These interesting properties, together with a clear indication that food-related PNFs are not harmful to consumer health (Lassé et al., 2016), make PNFs a good candidate for generating new

* Corresponding author.
E-mail address: anja.herneke@slu.se (A. Herneke).

https://doi.org/10.1016/j.foodhyd.2022.108315
Received 8 April 2022; Received in revised form 10 November 2022; Accepted 12 November 2022
Available online 14 November 2022

food applications with interesting functional properties.

Among plant-based proteins, soybean PNFs are the most widely researched due to soybean's long history of use in food products such as tofu and its good amino acid profile, comprising accurate amounts of essential amino acids (Akkermans et al., 2007; Josefsson et al., 2019; Thrane, Paulsen, Orcutt, & Krieger, 2017). Studies have shown that PNFs can also be made from other plant-based protein sources (Josefsson et al., 2020; Li et al., 2019; Li et al., 2020; Munialo et al., 2014). Among these, mung bean (*Vigna radiata*) is a promising candidate due to interesting morphological attributes of the protein nanofibrils (Herneke et al., 2021; Liu & Tang, 2013).

Mung bean is a commonly consumed legume in many Asian and African countries. Mung bean protein is a by-product from vermicelli (glass noodle) production, which is widespread in some Asian countries (Charoensuk, Brannan, Chanasattru, & Chaiyasit, 2018), and thus the protein is available for use in new sustainable food applications. Mung bean has a total protein content of 17–26% and a major proportion of the protein belongs to the family of globulins, which comprises three fractions (7S, 8S and 11S), divided according to their solubility (Mendoza, Adachi, Bernardo, & Utsumi, 2001). In mung bean protein, 8S is the major globulin fraction, constituting approximately 89% of the total globulin fraction. A study by Liu and co-workers comparing the functional properties of 8S globulins from 15 different cultivars concluded that these globulins showed diversity in functional properties and that the solubility, foaming capacity and foaming stability were highly pH-dependent. The lowest foaming capacity and stability were observed around pH 5 (i.e. close to the isoelectric point, IP), and the highest at pH 7 (Liu, Liu, Yan, Cheng, & Kang, 2015).

In an earlier study, our research group characterised the secondary structure and morphological properties of PNFs made from whole mung bean protein isolate (MPI) (Herneke et al., 2021). In the same study, we found that PNFs made from the extracted 8S fraction had higher amounts of β-sheets and were longer than PNFs made from the whole mung bean isolate. The PNFs generated from the 8S fraction were over 1 μm long and had curly morphology. A previous study by Loveday, Su, Rao, Anema, and Singh (2012) comparing PNFs made from β-lactoglobulin with two distinctly different morphologies (curly and straight) found that the curly PNFs had much higher viscosity than straight PNFs at the same concentration. These characteristics make curly PNFs a better candidate for use as thickener/gelators in a food system. Mung bean PNFs have these interesting characteristics and are made from a plant-based source, making mung bean PNFs an interesting candidate for use in future sustainable/vegan food applications. For future food applications to be identified, there is a need to understand how PNFs behave at food-related pH (~pH 4.0–7.0) and if/how pH changes their functional properties. Effects of pH on PNF structure has been documented previously for β-lactoglobulin (Kroes-Nijboer et al., 2012) and soybean (Wan & Guo, 2019), with reported aggregation of the PNFs around the isoelectric point (IP) of the original proteins.

This study comprised three tasks: (I) Optimising the conditions for generating mung bean- PNFs from whole protein isolate (MPI) and the 8S fraction, using thioflavin T (ThT) fluorescence assay, electrophoretic gel separation, circular dichroism (CD) spectroscopy and atomic force microscopy (AFM). (II) Determining the stability of PNFs made from MPI at increasing pH (2–9), using ThT, AFM and viscosity profiling. (III) Comparing foam formation capacity and stability for non-fibrillated and fibrillated MPI at pH 2–8.

2. Materials and methods

2.1. Material

Mung bean (*Vigna radiate*) cultivated in Myanmar was kindly provided by Lantmännen (Sweden). Hydrochloric acid (HCl) was procured from VWR (France), sodium chloride (NaCl) from VWR (Belgium), and thioflavin T (ThT) from Sigma (India).

2.2. Extraction of whole isolate from mung bean and the 8S fraction

Mung beans frozen in liquid nitrogen were milled in an ultra-centrifugal mill (ZM-1, Retsch GmbH, Germany) with a 500 μm mesh. The flour was dispersed in deionised water at a ratio of 1:10 (w/w) at 20 °C. The pH of the mixture was adjusted to 8.1 using 2 M NaOH. The mixture was then incubated with stirring at room temperature (20 ± 2 °C) for 1 h, followed by centrifugation at 3700*g* for 30 min. The supernatant was collected, pH-adjusted to 4.6 using 2 M HCl and incubated with continuous stirring for 1 h, and then centrifuged at 3700 g (20 °C, 15 min). The pellet was collected and dispersed in deionised water with 0.6 M NaCl and incubated with continuous stirring for 30 min. The supernatant was diluted in one step to 0.1 M NaCl to get the whole protein isolate. To get the 8S fraction, the supernatant was diluted in two steps, first to 0.35 M NaCl followed by centrifugation at 3700*g* for 15 min and then the supernatant was further diluted to 0.2 M NaCl and the pH was adjusted to 4.6. Centrifugation at 5000*g* was performed and the pellet was collected and dissolved in 0.01 M HCl, after which the pH was adjusted to 2. The sample was then dialysed, with 6–8 kDa molecular weight cut-off, for 24 h in 0.01 M HCl. The pH of the sample was once more adjusted to 2, if needed, and the sample was filtered through a 0.45 μm nylon syringe filter (Merck Millipore, Ireland). For protein extraction summery see diagram in appendix (Fig. A1). The protein content was measured with Kjeldahl to 89.3% for MPI and 90.1% for 8S for one extraction. The protein contents of the following protein extraction made with the same protocol were estimated by dry weight measurement after drying at 105 °C for 3 h.

2.3. Solubility curve for mung bean protein

After protein extraction, the sample was dialysed against water. The pH was then adjusted to 2.0 and the sample was again dialysed against 0.01 M HCl at pH 2.0. A 50 mL aliquot of this protein solution was placed in a beaker and the pH was gradually increased by addition of 1 M NaOH. At each pH step, 1 mL of sample was removed, placed in an Eppendorf tube and centrifuged at 9000 g for 10 min. The absorbance of each sample was measured at 280 nm.

2.4. SDS-PAGE

To compare the protein profiles of the whole protein isolates and the 8S fraction, SDS-PAGE was performed on Mini-PROTEAN TXG, 4–20% gels (Bio Rad). The samples were run under reducing conditions.

2.5. Preparation of protein nanofibrils from mung bean protein isolate and the 8S fraction

The protein concentration was adjusted to 25 mg/mL using 0.01 M HCl, the pH was adjusted to 2 and the samples were incubated in an oven at 85 °C for 24 h. The fibrillated samples were dialysed for 24 h with a 100 kDa membrane (Spectrum Laboratories Inc.). Approximately 44% of the protein was converted to PNFs (estimated by dry weight measurements).

2.6. Separation of protein nanofibrils and peptides

Separation of peptides and PNFs was performed using a previously described method (Kroes-Nijboer et al., 2012; Akkerman et al., 2007; . Wan et al., 2016). The fibrillated solution was diluted to 2 mg/mL with 0.01 M HCl. The solution was divided into centrifugal filter tubs with 100 kDa molecular weight cut-off (Viva Spin 20, Sartorius) and centrifuged at 3000 g for 15 min. This process was repeated four times and the filtrate was recovered after each centrifugation, while the retentate was recovered after the last centrifugation. The protein concentration in the retentate and filtrate was calculated by dry weight measurements, according to which the fibrillated solution consisted of 48% PNFs.

2.7. Thioflavin T fluorescence

Thioflavin T fluorescence assay was used to detect formation of amyloid-like PNFs. A ThT stock solution of 1 mM was prepared by diluting ThT in phosphate buffer (10 mM phosphate, 150 mM NaCl, pH 7.0). The stock solution was filtered through a 0.2 μm nylon syringe filter (VWR, USA) and stored covered in aluminium foil at −21 °C. On the day of analysis, the stock solution was diluted in phosphate buffer to make a 50 μM working solution. A 100 μL sample was mixed with 900 μL of the ThT working solution and incubated for 20 min at room temperature before testing. Fluorescence intensity was measured using a multi-mode microplate reader (Polarstar Omega, BMG Labtech, Germany) at an excitation wavelength of 440 nm (slit width = 10.0 nm) and an emission wavelength of 480 nm (slit = 10.0 nm). The ThT working solution without addition of a protein sample was used as a blank.

2.8. Circular dichroism spectroscopy

The CD measurements were performed according to the method and instrument described and used in our earlier work (Herneke et al., 2021). In short, the sample concentration was adjusted to 0.1 mg/mL and the spectra were obtained at 25 °C for the range 190–270 nm, with an optical path length of 1 mm. The spectral resolution was 1 nm, with a response time of 1 s at a bandwidth of 2 nm. Ten scans were accumulated and averaged, and the baseline (0.01 M HCl) was subtracted.

2.9. Sample preparation and pH adjustment

The PNF samples made from MPI were diluted to 1 mg/mL with 0.01 M HCl. The pH was adjusted to 3, 4, 5, 6, 7, 8, and 9 with 0.1, 0.5, and 1 M NaOH. The samples were incubated overnight at 4 °C before being analysed with ThT and AFM.

2.10. Atomic force microscopy

Atomic force microscopy imaging was carried out using a Bruker Dimension FastScan instrument operating in fast scan mode. The samples were diluted between 1:50 and 1:1000 in 0.01 M HCl, and 10–15 μL were applied on freshly cleaved mica surfaces and dried in air. FastScan B cantilevers from Bruker were used for the experiments and the micrographs were analysed with Gwyddion 2.48 (http://gwyddion.net/).

2.11. Rheological measurements

Steady shear measurements of pH-adjusted samples were carried out using a DISCOVERY HR-3 hybrid rheometer (DHR3) (TA Instrument, USA) with a cone plate geometry (40 mm diameter, cone angle 2°, 51 μm). The shear rate was increased from 0.1 to 500 s^{-1} and the viscosity (η) was recorded. All measurements were carried out at 25 °C and repeated at least three times.

2.12. Foaming properties

A 20 mL portion of 15 mg/mL protein/PNF solution was transferred to a wide-necked 250 mL measuring cylinder. The separated PNFs and peptides had a volume of 16 mL and a concentration of 0.98 mg/mL. The probe of an Ultra Turrax t 25 homogeniser was immersed in the solution, the homogeniser was started and the speed was gradually increased from 8000 rpm to 13 500 rpm. The solution was allowed to foam for a total of 5 min and the foam volume was recorded.

The foam volume was recorded after 15, 30, 120, and 360 min standing at room temperature. The foam stability (FS) after a specific duration and the foam capacity (FC) were determined using the following equations:

$$FS = FV_t \,/\, FV_i \times 100 \quad (1)$$

$$FC = FV_i \,/\, V_i \times 100 \quad (2)$$

where V_i is the volume of protein solution before whipping, FV_i is the foam volume at time zero, and FV_t is the volume of foam at time t.

The foam half-life was determined according to the exponential decay law:

$$H(t) = H(0)\exp(-\lambda t) \quad (3)$$

where H(t) is the foam height at time t, H0 is the initial foam height at time t = 0 and λ (lamda) is the decay constant. This exponential relationship can be converted to a linear equation by taking the natural logarithm of the foam height ln(H(t) versus time:

$$\ln(H(t) = \ln(H(0)) - \lambda t \quad (4)$$

The half-life ($t_{1/2}$) of the foams was determined using the following equation:

$$t_{1/2} = \ln(H(t_{1/2}) - \ln(H(0)) \,/\, -\lambda \quad (5)$$

2.13. Confocal microscopy

To investigate the surface structure of non-fibrillated and fibril-stabilised foam, a confocal laser scanning microscope (CLSM; Zeiss LSM 780, Jena, Germany), built on an inverted Zeiss Axio Observer and supersensitive GaASp detector, was used. The foams from PNFs and MPI (1 mL) were transfer and placed on the concave microscope slide using 1 mL Eppendorf pipette with head-cut tip. Fluorescence dye of ThT (10 μL with the concentration of 3 mM, dispersed into phosphate-buffered saline 10 mM PBS, pH 6.8) was added to the microscope slide to probe protein distribution in foams. ThT fluorescence was excited with an Argon laser (488 nm) and emission wavelengths between 500 nm and 530 nm were detected. All images were acquired using a C-Apochromat 63× oil immersion objective (1.32 NA) with resolution 1024*1024 pixels. The distribution of bubble ferret diameter and area fraction in each sample were processed using the software Image J. Image calibration was required to correlate the image dimensions in pixels to physical dimensions. Image processing algorithms require a binary image that can be produced by applying an appropriate threshold. Seven images in each sample were used to calculate the average of bubble ferret diameter and area fraction in foam.

3. Results and discussion

3.1. Mung bean-based PNFs from whole protein isolate and the 8S fraction

Formation of PNFs from both mung bean protein (MPI) and 8S was investigated after 0, 2, 4, 6, 24 and 48 h of heat treatment at 85 °C, using ThT fluorescence assay and electrophoretic gel separation (Fig. 1A and B). The two protein samples showed similar fibrillation kinetics according to ThT fluorescence (Fig. 1A), with a strong increase in average relative fluorescence intensity (~100 000 a.u) after 2 h of heat treatment. The average relative fluorescence intensity decreased over time for both heat-treated proteins and was lowest (~70 000 a.u) after 48 h of heat treatment.

Analysis of the samples on an electrophoretic gel revealed that the MPI sample had bands corresponding to the bands observed for the 8S fraction before heating, plus additional bands indicating presence of 7S and 11S globulins (Fig. 1B). For the sample containing 8S, four bands were observed. These bands corresponded closely to the molecular weights reported by Mendoza et al. (2001) for the four subunits of 8S (64, 48, 32, 26 kDa), indicating that this sample consisted of the globular fraction, as expected. Presence of shorter peptides was observed for both samples after heating for 2–6 h. When both MPI and 8S had been heat-treated for 24 h, only small peptide fractions were detected in the

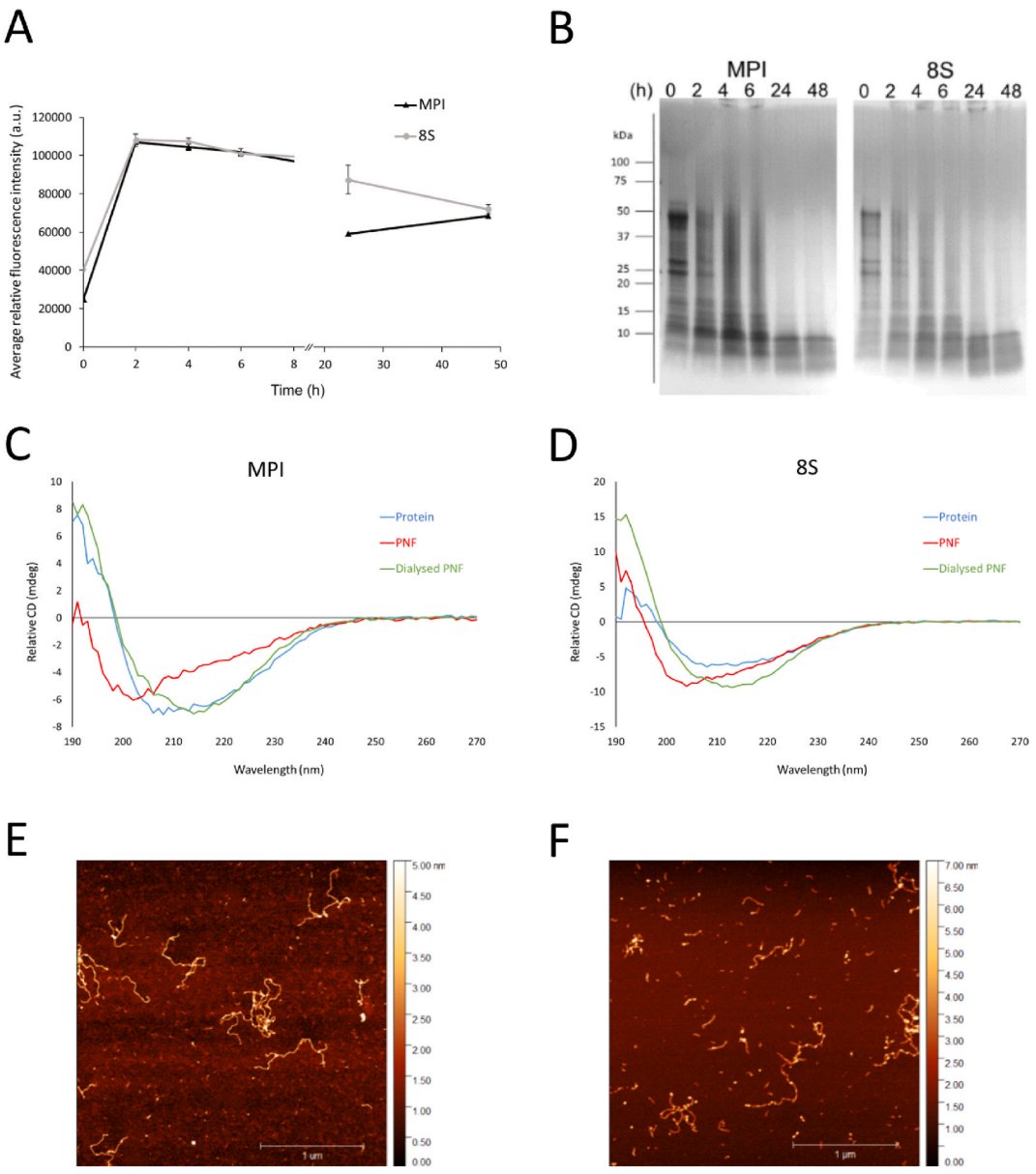

Fig. 1. (A) Average relative ThT fluorescence intensity of MPI and 8S protein samples at a concentration of 25 mg/mL after 0, 2, 4, 6, 24 and 48 h of heating (85 °C) at pH 2. (B) Electrophoretic pattern of MPI and 8S protein samples after 0, 2, 4, 6, 24 and 48 h of heating (85 °C) at pH 2. (C, D) Circular dichroism spectra of non-fibrillated protein (blue), PNFs (red), and dialysed protein nanofibrils (PNFs) (green) from MPI and the 8S fraction. Atomic force microscopy image of PNFs from (E) MPI and (F) 8S after 24 h of heating. (For interpretation of the references to colour in this figure legend, the reader is referred to the Web version of this article.)

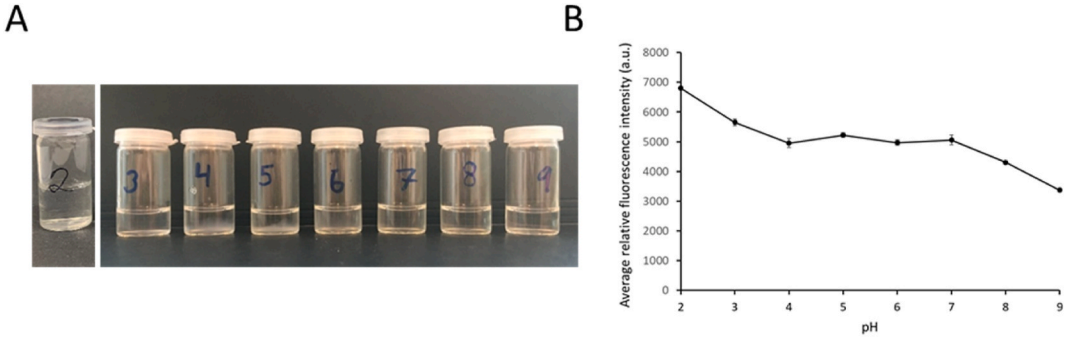

Fig. 2. (A) Visual appearance of protein nanofibrils (PNFs) made from MPI (1 mg/mL) at pH 2–9. (B) Change in average relative ThT fluorescence intensity at increasing pH for PNFs made from MPI.

samples. These results are in line with findings in a previous study on formation of PNFs from MPI and 8S fraction, which concluded that it takes at least 12 h before a fibrillary structure can be observed with AFM (Liu & Tang, 2013).

On comparing the secondary structure with CD spectroscopy for non-fibrillated samples (protein), 24 h heat-treated protein samples (PNF), and dialysed fibrillated samples ('dialysed PNF') from both MPI and 8S (Fig. 1C and D), it was found that the samples behaved similarly. A shift to more β-sheet structures was observed for both MPI and 8S after dialysis, indicating that the fibrillated samples from both proteins had the characteristic profile for PNFs with a high amount of β-sheets. The reason that the non-dialyzed samples (PNF) had a more disordered structure is probably because small peptides were still present in the sample, but later removed by the dialysis process. The morphology of the dialysed PNFs from both samples was investigated with AFM (Fig. 1E–F, Fig. A2A-B). The PNFs in the fibrillated MPI and 8S samples had a similar curly structures and length of ~1 μm. Compared with the fibrillated MPI examined in our earlier study (Herneke et al., 2021), the MPI in this study was further purified with the help of salt extraction, which generated a more pure protein isolate. This is probably the reason why the fibrillated MPI in this study behaved very similarly to the 8S sample. Since there was less work in extracting MPI compared with 8S and since total protein yield was higher (13–21% for MPI and 9.9–15% for 8S), in this study we further evaluated PNFs from MPI.

3.2. Stability and morphology at increasing pH of PNFs made from MPI

The dialysed fibrillated MPI solution was diluted to a concentration of 1 mg/mL and divided into eight different samples, in which the pH was increased from 2 to 3, 4, 5, 6, 7, 8, or 9 with NaOH. Between pH 4–6, the samples had a cloudy appearance (Fig. 2A). The IP of native mung bean protein is around pH 4.6, which also seemed to apply for PNFs made from MPI. Similar findings have been reported for pure PNFs based on β-lactoglobulin, with samples having a cloudy appearance around the IP of the native protein (Kroes-Nijboer et al., 2012; Peng et al., 2017). On investigating the average relative ThT fluorescence at pH 2–9 (Fig. 2B), a small drop in fluorescence was observed already at pH 3. On reaching pH 4, the fluorescence decreased further but then stabilised until pH 8, after which point the fluorescence dropped once again to reach its lowest value at pH 9. The proposed mechanism of the ThT dye is that it binds to the surface side-chain grooves that run parallel to the long axis of the fibrils (Biancalana & Koide, 2010). The drop in fluorescence can probably be correlated to degradation of PNFs, as observed with the help of AFM (Fig. 3). It should be borne in mind that the ThT dye was diluted in phosphate buffer at pH 7 and, even though the samples were only incubated for 20 min, this might have affected the accuracy when using ThT assay to measure the influence of changes in pH on the PNFs. For that reason, further analysis of how the PNFs were affected by increasing pH was performed using AFM imaging (Fig. 3).

At pH 3, the PNFs still had a similar structure to the original pH (2), but they were slightly shorter and smaller PNF fragments were detected in the sample. The amount of shorter PNFs increased at pH 4. Between pH 5–6, the PNFs appeared to be more aggregated, which was expected due to the cloudiness observed in the samples at this pH (see Fig. 2A). At pH 7, the PNFs seemed to be slightly shorter than at the original pH, but they still had the original curly structure and no aggregation was observed in the samples. At pH 8, the PNFs looked entangled but still had their characteristic curly PNF morphology. This characteristic structure disappeared at pH 9, and the sample consisted of smaller aggregates. These results are in agreement with previous findings on the effect of pH on PNFs from β-lactoglobulin (Kroes-Nijboer et al., 2012; Gilbert, Campanella, & G. Jones, 2014; Peng et al., 2017) and soybean (Wan & Guo, 2019), where aggregation of the PNFs were observed around the IP of respective protein due to electrostatic net charge and at pH above the IP the PNFs get a negative charge which facilitated disintegration of the fibrillary β-sheet rich structure.

3.3. MPI and PNFs ability to form and stabilise foams at pH 2-8

Viscosity profiles for non-fibrillated MPI and fibrillated MPI (not dialysed) at pH 2–8 as a function of shear rate are presented in Fig. 4. The fibrillated samples at any given pH had much higher viscosity (0.044–20.005 Pa s) than the corresponding non-fibrillated samples (0.002–0.384 Pa s) at a low shear rate (0.1 s^{-1}) and the same concentration (Fig. 4A and B). The viscosity was highest for the fibrillated samples at pH 4, followed by pH 5 at low shear rates (Fig. 4B). Similar findings have been reported by Peng et al. (2017) for β-lactoglobulin PNFs, who observed the highest viscosity for samples at pH 5, followed

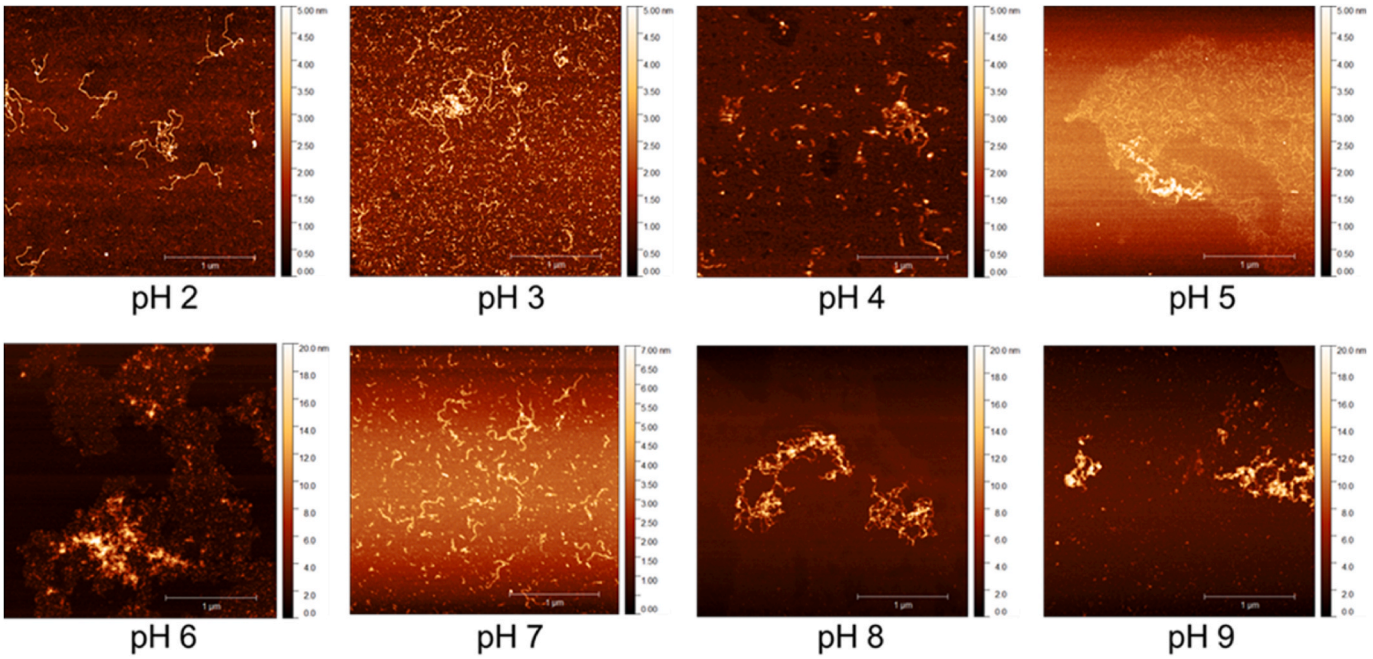

Fig. 3. Atomic force microscopy images of protein nanofibrils (PNFs) made from MPI at pH 2–9.

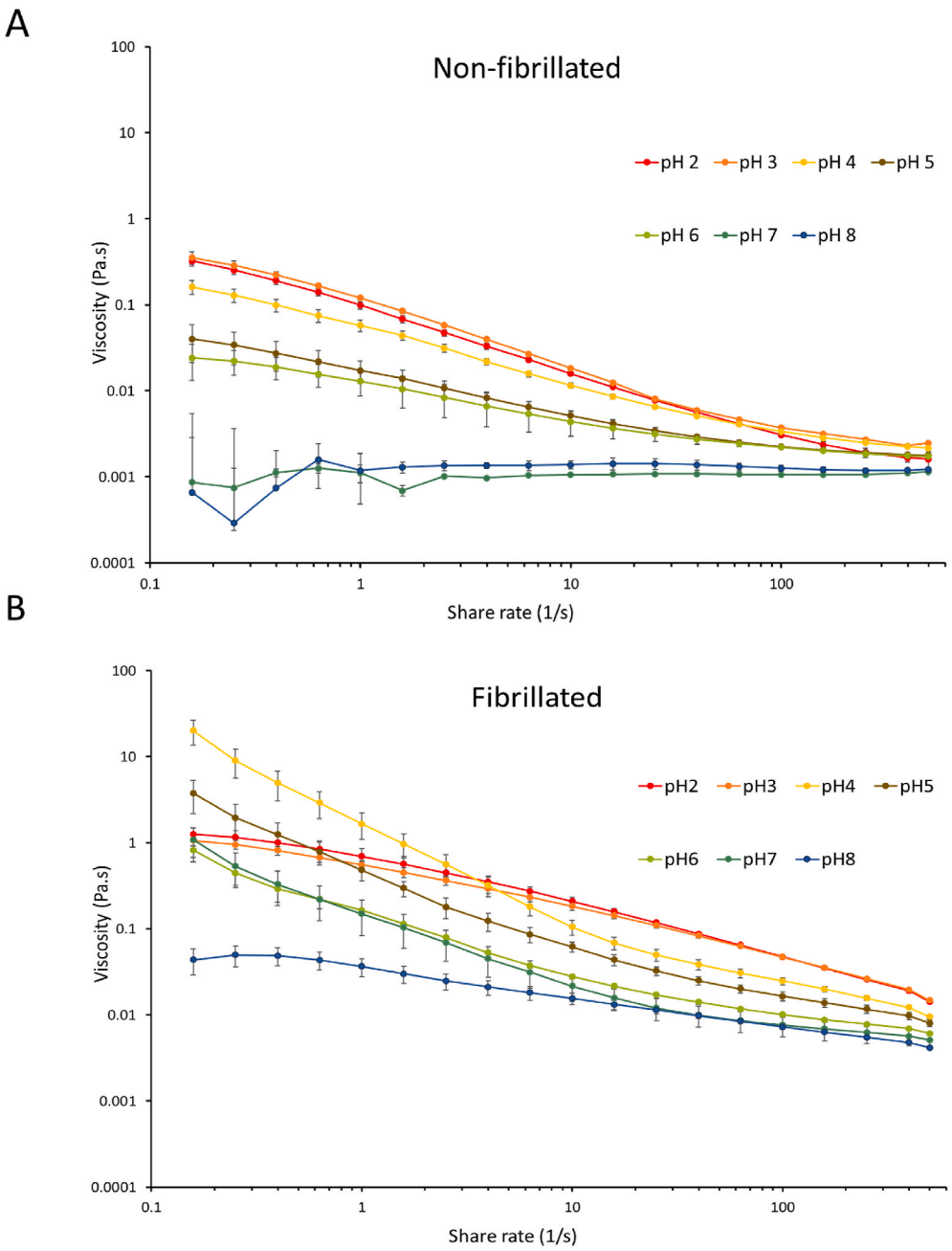

Fig. 4. Viscosity (Pa.s) versus shear rate (0.1–500 s^{-1}) for (A) non-fibrillated and (B) fibrillated protein at pH 2–8 (conc. 15 mg/mL).

by pH 4 and 6. This behaviour is expected due to increased attractive forces of the PNFs around the IP of the protein, and can be linked to the aggregation of PNFs observed with AFM at the same pH (see Fig. 3). All samples showed shear-thinning behaviour when the shear rate increased from 0.1 to 500 s^{-1}. The fibrillated samples at pH 2 and 3 had lower viscosity at a low shear rate than those at pH 4 and 5. However, the decrease in viscosity at the increased shear rate was not as steep for the samples at pH 2 and 3 as for the other samples. This might be due to the specific morphology of mung bean PNFs, with the long and curly structure that was still present at this particular pH making the PNFs more resistant to increased shear. The viscosity profiles of the PNFs made from MPI were different to those reported for PNFs made from β-lactoglobulin at the same pH (Peng et al., 2017). This difference might be because the PNFs from β-lactoglobulin were straight instead of curly, making them less prone to form a network and resulting in less resistance to shear than mung bean PNFs. As stated earlier, curly PNFs from β-lactoglobulin have been reported to have much higher viscosity, particularly at a higher shear rate, than straight PNFs from the same source and concentration (Loveday et al., 2012).

Foams of the native protein (non-fibrillated) and heated MPI (fibrillated) were generated by intense mixing with a homogeniser. This intense mixing caused the PNFs to become shorter but the curved morphology remained (Fig. A3). Foaming properties (foam capacity and foam stability) were evaluated over a time interval of 15–360 min at pH 2–9 (Fig. 5). The non-fibrillated and fibrillated samples both showed an increase in foam volume at all pH values tested after the homogenisation process. However, the increase in foam volume for the fibrillated samples was between 40% and 110% higher than for the non-fibrillated samples. The greatest difference in foam volume increase was at pH 4, at which the fibrillated samples showed a 500% foam volume increase, compared with 222% for the non-fibrillated samples (Fig. 5A). At pH 4 and 7, the fibrillated samples generated much more stable foams

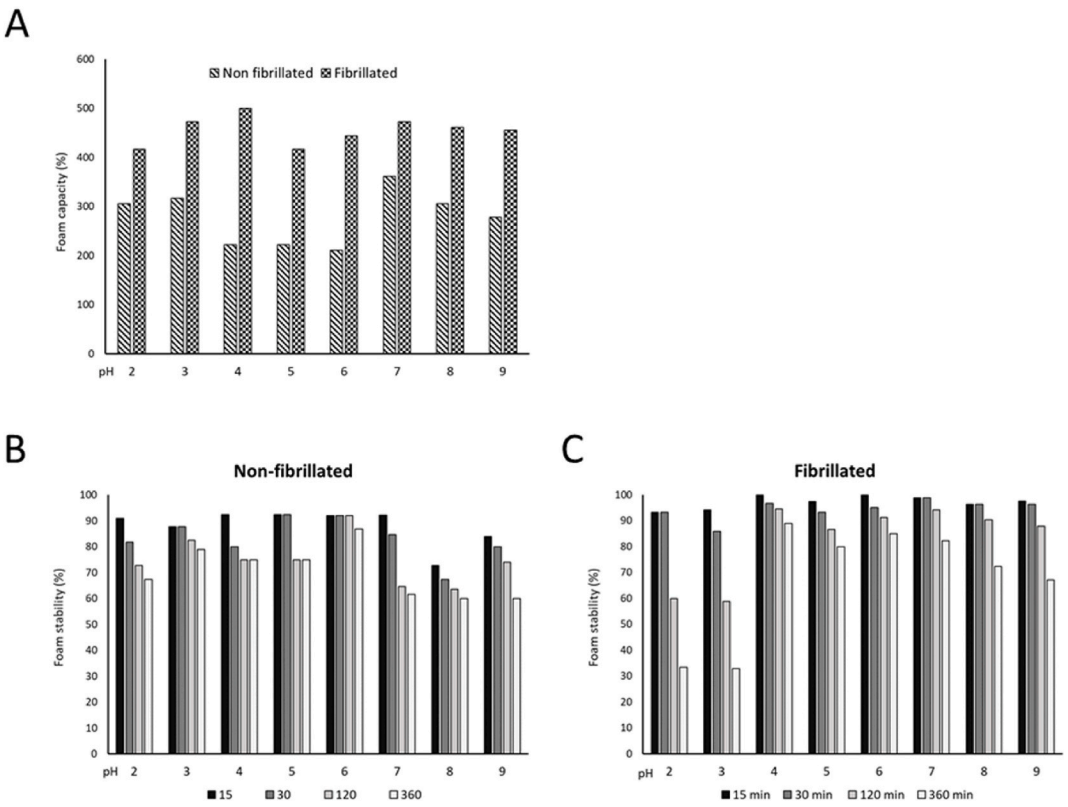

Fig. 5. Fibrillated and non-fibrillated MPI analysed for (A) foam capacity and (B, C) foam stability at pH 2–9.

compared with the non-fibrillated samples (Fig. 5B–C, Fig. A4), which is promising because most food systems function at pH 4–7. At low pH (2–3) and at pH 6, foam stability was greater for the non-fibrillated samples than for the fibrillated samples. The estimated half-life time for the foams from both the non-fibrillated and fibrillated samples at pH 6, where 2143.9 and 1693.8 min, respectively (Fig. A4). The reason why the non-fibrillated samples were more stable at this pH than the fibrillated samples is not fully clear. It might be because of errors in the data contributing to poor fitting of the model ($R^2 = 0.6138$). At pH values above 7, the foams made from the fibrillated samples were once more less stable, but still more stable than those from the non-fibrillated samples.

There are several possible explanations as to why the foam properties of non-fibrillated samples were inferior to those of fibrillated samples. For instance, the major protein (8S fraction) is highly ordered (Tang & Sun, 2010), which makes the structure inflexible. The 8S fraction has N-linked glycans, which also might contribute to lower surface hydrophobicity (Garcia, Adachi, Tecson-Mendoza, Bernardo, & Utsumi, 2006). These are all properties that contribute to lower foam capacity and foam stability. However, compared with earlier reports on foaming properties of mung bean protein, the non-fibrillated samples also had higher foam capacity (Butt & Batool, 2010; El-adawy, 2000; Brishti et al., 2017). This could be due to several factors, such as protein concentration, purity of the protein or how the protein solution was treated. The protein isolate in this study was exposed to the same treatment as the fibrillated samples, except for the heat incubation. Exposing the protein to low pH (2) probably caused partial disruption of the quaternary protein structure, generating smaller particles and exposing hydrophobic sites that might improve the foam capacity and foam stability (Jiang, Wang, & Xiong, 2018).

In this study, the foaming experiments were performed on the mixture of PNFs and small peptides still present in the sample after 24 h heating at 85 °C. It was not fully clear from the data whether the PNFs or the small peptides contributed most to the improved foaming ability of the fibrillated samples. This issue was investigated for PNFs made from the 11S globular fraction of soybean in a study by Wan et al. (2016). Those authors compared the foaming properties of samples containing a mixture of PNFs and peptides, purified PNFs and peptides separated by filtration at pH 2, 5 and 7, and concluded that purified PNFs had the poorest foaming properties. However, Peng et al. (2017) found that PNFs made from β-lactoglobulin with the small peptides removed generated more stable foams around the IP than untreated protein in the same conditions. These results are contradictory and further studies are needed to clarify whether PNFs or peptides in the heat-treated protein are responsible for the improved foaming properties.

To investigate further which fraction of the fibrillated MPI samples that contributed most to stabilising the foams, the peptides and PNFs were separated with the help of spin membranes according to the method described by Wan et al. (2016). ThT fluorescence measurements on the sample before filtration (PNFs + peptides), the retentate (pure PNFs), and filtrates (W1–W4) showed that the fluorescence intensity was approximately 100 times higher in the original sample and retentate than in the filtrates, indicating that no PNFs were present in the filtrates (Fig. 6A). The foaming capacity of the fibrillated samples before filtration, the retentate and the first filtrate (W1) were investigated at pH 2, 5 and 7 (Fig. 6B). The first filtrate had the lowest foaming capacity at all pH values, and gave the least stable foams at pH 5 and 7 (Fig. 6C).

These findings suggest that mung bean PNFs contribute to enhanced foam stability, and not the peptides. These results contradict conclusions by Wan et al. (2016) on soybean PNFs. The reason for this discrepancy is not clear, but it might derive from structural differences in PNFs from soybean 11S and mung bean, as the PNFs from 11S have a straight, semi-flexible structure and the PNFs from mung bean have a much more curly, flexible structure.

Confocal microscopy was used to image the foams of non-fibrillated and fibrillated MPI at pH 2–8 at time 0 (Fig. 7A). As stated earlier, the foaming capacity of fibrillated samples was better than that of non-fibrillated samples at all pH values (see Fig. 5A). Both non-fibrillated

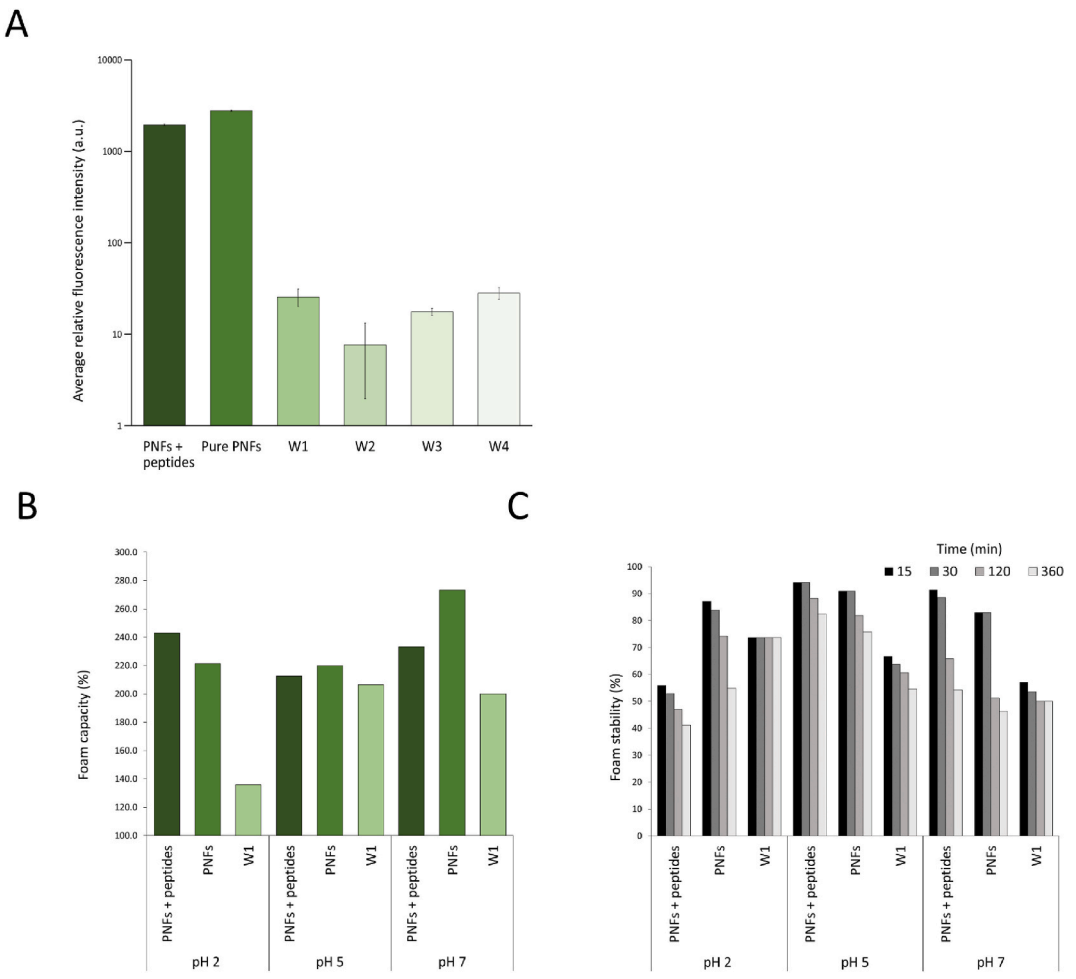

Fig. 6. (A) Average relative fluorescence intensity of the original sample before filtration (PNF + peptides), the retentate (Pure PNFs), and the filtrate after the first, second, third and fourth wash (W1–W4). (B) Foam capacity and (C) foam stability (measured for 0–360 min) for samples with PNFs + peptides, PNFs and W1 at pH 2, 5 and 7.

and fibrillated samples had a high frequency of small bubbles (10–50 μm) (Fig. 7B). However, the fibrillated samples had a more uniform distribution of these small bubbles (Fig. B) than the non-fibrillated samples, which had a large quantity of small bubbles between 10 and 20 μm (Fig. 7B).

At pH 2 and 3, the fibrillated samples had low foam stability (see Fig. 5C). This can be explained by the higher frequency of large bubbles than in fibrillated samples at higher pH (Fig. 7B), indicating faster merging of bubbles. When the pH increased (pH 4–9), the stability of the foams made from fibrillated samples improved (Fig. 5C, Fig. A1), and a greater fraction of small bubbles was detected in these samples compared with the samples at lower pH (Fig. 7B). These results are in line with earlier findings on foam properties of whey PNFs, where foams made with PNFs at pH 7 were more stable and had a lower frequency of large bubbles than foams made with PNFs at pH 2 (Oboroceanu et al., 2014).

The non-fibrillated samples had the best foaming capacity at pH 2, 3, 7 and 8 (see Fig. 5A), and had a mixture of small and large bubbles ('Non-fibrillated' section in Fig. 7A). For non-fibrillated samples, the ratio of small to large bubbles varied proportionally to the solubility of the samples (Fig. 7B, Fig. A5). Low solubility generated samples with a larger fraction of large bubbles, and high solubility generated samples with a larger fraction of small bubbles.

Area fraction measurements were made of the green fluorescence ThT dye coverage in each image (Fig. 7D). All micrographs were imaged at the bottom of the foams. The larger area fraction for non-fibrillated samples at pH 2, 3, 7 and 8 can be explained by the larger number of small bubbles compared with the fibrillated samples. The larger area fraction for non-fibrillated samples close to the IP of mung bean protein (pH 5 and 6) can be explained by large aggregates accumulating at the bottom of the foams. These large aggregates probably explain why the non-fibrillated samples had low foam capacity (see Fig. 5A) around pH 4–6. At pH 6, the non-fibrillated samples started to move away from the IP and the aggregates probably became smaller, which helped to improve the foam stability (Fig. 5B, Fig. A4).

ThT dye assay is a standard method to detect β-sheet rich structures such as PNFs (Biancalana & Koide, 2010). The ThT dye also binds to non-fibrillated samples ('Non-fibrillated', Fig. 7A), probably due to the presence of β-sheets in the untreated MPI, as shown in Fig. 1A at 0 h of heat treatment. However, fibrillated samples had a stronger green colour ring around the bubbles than non-fibrillated samples ('Fibrillated', Fig. 7A), indicating a thicker film around the bubbles. Hence the PNFs appeared to be more surface active than the non-fibrillar protein. This is probably one of the reasons why fibrillated samples created generally more stable foams.

4. Conclusions

This study demonstrated that PNFs formed from the whole protein isolate of mung bean, consisting of three different globular fractions, are very similar in terms of secondary structure and morphology to PNFs generated from the major globulin 8S fraction from the same bean. On

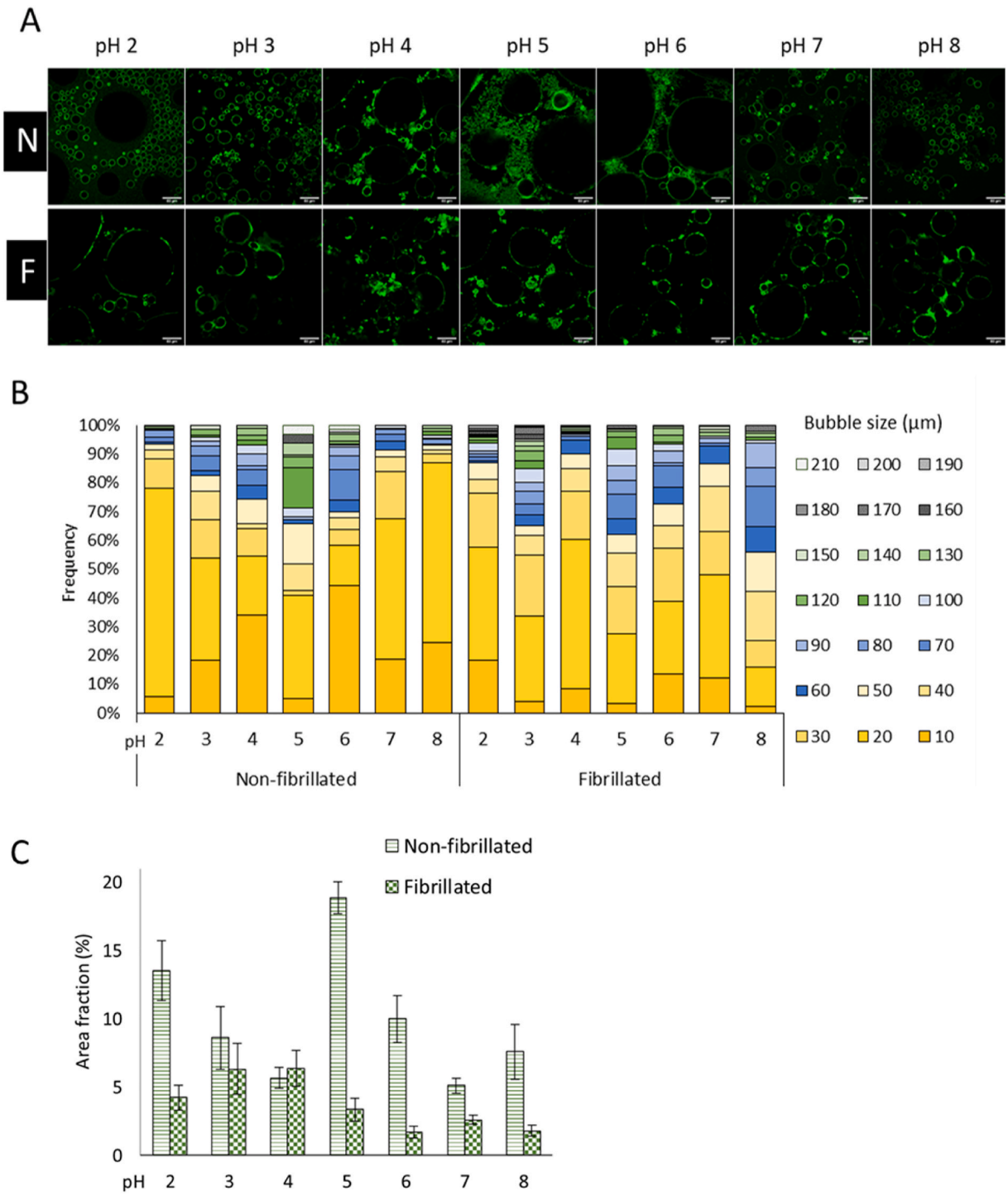

Fig. 7. (A) Confocal images of bubbles stabilised by non-fibrillated (N) and fibrillated (F) MPI at different pH (2–8), scale bar 50 μm stained with THT fluorescence dye. (B) Distribution of bubble size (from 10 to 210 μm, the size displayed is the highest value and increases +10 μm at a time) in foams made from non-fibrillated and fibrillated samples at different pH. (C) Area fraction (%) of the green fluorescence ThT dye in each image of foams from non-fibrillated and fibrillated samples at different pH. (For interpretation of the references to colour in this figure legend, the reader is referred to the Web version of this article.)

exposure of PNFs from the whole isolate to increasing pH, the morphology of the PNFs changed. Aggregation of the PNFs was detected around pH 4–6 and at pH 7 the fibrils still had their curly structure, but were not as long as at the original pH (2). A major novel finding in this study is that PNFs made from purified mung bean protein are a promising candidate for use as foam stabilisers.

The results obtained in this study provide a deeper understanding of how to optimise production of PNFs from mung beans, how these PNFs may behave at food-related pH values and how they can be used in food model systems such as foams. This brings us one step closer to understanding how plant-based PNFs, such as those from mung bean, can be used to produce new food applications with an attractive/tailored texture.

Author statement

Anja Herneke: Conceptualization, Formal analysis, Investigation, Writing - Original Draft, Visualization. **Saeid Karkehabadi:** Investigation, Writing - Review & Editing. **Jing Lu** Investigation, Formal analysis. **Christofer Lendel** Writing - Review, Editing, Supervision. **Maud Langton** Conceptualization, Writing - Review, Editing, Supervision.

Declaration of competing interest

The authors have declared no conflict of interest.

Data availability

Data will be made available on request.

Acknowledgments

This project was financially supported by Formas (grant no. 2018–01869), Lantmännen Research Foundation (grant no. 2017F003 and grant no. 2018F004), Trees and Crops for the Future (TC4F), a Strategic Research Area at SLU, supported by the Swedish Government, and the Faculty of Natural Resources and Agricultural Sciences at the Swedish University of Agricultural Sciences (SLU).

Appendix A. Supplementary data

Supplementary data to this article can be found online at https://doi.org/10.1016/j.foodhyd.2022.108315.

References

Akkermans, C., Van Der Goot, A. J., Venema, P., Gruppen, H., Vereijken, J. M., Van Der Linden, E., et al. (2007). Micrometer-sized fibrillar protein aggregates from soy glycinin and soy protein isolate. *Journal of Agricultural and Food Chemistry, 55*(24), 9877–9882. https://doi.org/10.1021/jf0718897

Akkerman, C., Van Der Goot, A. J., Venema, P., Gruppen, H., Vereijken, J. M., Van Der Linden, E., et al. (2007). Micrometer-sized fibrillar protein aggregates from soy glicinin and soy protein isolates. *Journal of Agricultural and Food Chemistry, 55*, 9877–9882.

Amagliani, L., & Schmitt, C. (2017). Globular plant protein aggregates for stabilization of food foams and emulsions. *Trends in Food Science & Technology, 67*, 248–259. https://doi.org/10.1016/j.tifs.2017.07.013

Biancalana, M., & Koide, S. (2010). Molecular mechanism of Thioflavin-T binding to amyloid fibrils. *Biochimica et Biophysica Acta, Proteins and Proteomics, 1804*(7), 1405–1412. https://doi.org/10.1016/j.bbapap.2010.04.001

Brishti, F. H., Zarei, M., Muhammad, S. K. S., Ismail-Fitry, M. R., Shukri, R., & Saari, N. (2017). Evaluation of the functional properties of mung bean protein isolate for development of textured vegetable protein. *International Food Research Journal, 24*(4), 1595–1605.

Butt, M. S., & Batool, R. (2010). Nutritional and functional properties of some promising legumes protein isolates. *Pakistan Journal of Nutrition*. https://doi.org/10.3923/pjn.2010.373.379

Cao, Y., & Mezzenga, R. (2019). Food protein amyloid fibrils: Origin, structure, formation, characterization, applications and health implications. *Advances in Colloid and Interface Science, 269*, 334–356. https://doi.org/10.1016/j.cis.2019.05.002

Charoensuk, D., Brannan, R. G., Chanasattru, W., & Chaiyasit, W. (2018). Physicochemical and emulsifying properties of mung bean protein isolate as influenced by succinylation. *International Journal of Food Properties, 21*(1), 1633–1645. https://doi.org/10.1080/10942912.2018.1502200

El-adawy, T. A. (2000). *Functional properties and nutritional quality of acetylated and succinylated mung bean protein isolate. 70* pp. 83–91).

Garcia, R. N., Adachi, M., Tecson-Mendoza, E. M., Bernardo, A. E. N., & Utsumi, S. (2006). Physicochemical properties of native and recombinant mungbean (Vigna radiata L. Wilczek) 8S globulins and the effects of the N-linked glycans. *Journal of Agricultural and Food Chemistry, 54*(16), 6005–6010. https://doi.org/10.1021/jf0605897

Gilbert, J., Campanella, O., & Jones, O. G. (2014). Electrostatic stabilization of β-lactoglobulin fibrils at increased pH with cationic polymers. *Biomacromolecules, 15*(8), 3119–3127. https://doi.org/10.1021/bm500762u

Herneke, A., Lendel, C., Johansson, D., Newson, W., Hedenqvist, M., Karkehabadi, S., et al. (2021). Protein nanofibrils for sustainable food–characterization and comparison of fibrils from a broad range of plant protein isolates. *ACS Food Science & Technology, 1*(5), 854–864. https://doi.org/10.1021/acsfoodscitech.1c00034

Jiang, J., Wang, Q., & Xiong, Y. L. (2018). A pH shift approach to the improvement of interfacial properties of plant seed proteins. *Current Opinion in Food Science, 19*, 50–56. https://doi.org/10.1016/j.cofs.2018.01.002

Josefsson, L., Cronhamn, M., Ekman, M., Widehammar, H., Emmer, Å., & Lendel, C. (2019). Structural basis for the formation of soy protein nanofibrils. *RSC Advances, 9*(11), 6310–6319. https://doi.org/10.1039/c8ra10610j

Josefsson, L., Ye, X., Brett, C. J., Meijer, J., Olsson, C., Sjögren, A., et al. (2020). Potato protein nanofibrils produced from a starch industry sidestream. *ACS Sustainable Chemistry & Engineering*. https://doi.org/10.1021/acssuschemeng.9b05865

Kroes-Nijboer, A., Sawalha, H., Venema, P., Bot, A., Flöter, E., Den Adel, R., et al. (2012). Stability of aqueous food grade fibrillar systems against pH change. *Faraday Discussions, 158*, 125–138. https://doi.org/10.1039/c2fd20031g

Lam, S., Velikov, K. P., & Velev, O. D. (2014). Pickering stabilization of foams and emulsions with particles of biological origin. *Current Opinion in Colloid & Interface Science, 19*(5), 490–500. https://doi.org/10.1016/j.cocis.2014.07.003

Lassé, M., Ulluwishewa, D., Healy, J., Thompson, D., Miller, A., Roy, N., et al. (2016). Evaluation of protease resistance and toxicity of amyloid-like food fibrils from whey , soy , kidney bean , and egg white. *Food Chemistry, 192*, 491–498. https://doi.org/10.1016/j.foodchem.2015.07.044

Li, J., Pylypchuk, I., Johansson, D. P., Kessler, V. G., Seisenbaeva, G. A., & Langton, M. (2019). Self-assembly of plant protein fibrils interacting with superparamagnetic iron oxide nanoparticles. *Scientific Reports, 9*(1), 1–18. https://doi.org/10.1038/s41598-019-45437-z

Liu, H., Liu, H., Yan, L., Cheng, X., & Kang, Y. (2015). Functional properties of 8S globulin fractions from 15 mung bean (Vigna radiata (L.) Wilczek) cultivars. *International Journal of Food Science and Technology, 50*(5), 1206–1214. https://doi.org/10.1111/ijfs.12761

Liu, J., & Tang, C. H. (2013). Heat-induced fibril assembly of vicilin at pH2.0: Reaction kinetics, influence of ionic strength and protein concentration, and molecular mechanism. *Food Research International, 51*(2), 621–632. https://doi.org/10.1016/j.foodres.2012.12.049

Li, T., Wang, L., Zhang, X., Geng, H., Xue, W., & Chen, Z. (2020). Assembly behavior, structural characterization and rheological properties of legume proteins based amyloid fibrils. *Food Hydrocolloids, 111*(October 2020), Article 106396. https://doi.org/10.1016/j.foodhyd.2020.106396

Loveday, S. M., Su, J., Rao, M. A., Anema, S. G., & Singh, H. (2012). Whey protein nanofibrils: The environment-morphology-functionality relationship in lyophilization, rehydration, and seeding. *Journal of Agricultural and Food Chemistry, 60*(20), 5229–5236. https://doi.org/10.1021/jf300367k

Mendoza, E. M. T., Adachi, M., Bernardo, A. E. N., & Utsumi, S. (2001). Mungbean [vigna radiata (L.) wilczek] globulins: Purification and characterization. *Journal of Agricultural and Food Chemistry, 49*(3), 1552–1558. https://doi.org/10.1021/jf001041h

Munialo, C. D., Martin, A. H., Van Der Linden, E., & De Jongh, H. H. J. (2014). Fibril formation from pea protein and subsequent gel formation. *Journal of Agricultural and Food Chemistry, 62*(11), 2418–2427. https://doi.org/10.1021/jf4055215

Murray, B. S. (2020). Recent developments in food foams. *Current Opinion in Colloid & Interface Science, 50*. https://doi.org/10.1016/j.cocis.2020.101394

Oboroceanu, D., Wang, L., Magner, E., & Auty, M. A. E. (2014). Fibrillization of whey proteins improves foaming capacity and foam stability at low protein concentrations. *Journal of Food Engineering, 121*(1), 102–111. https://doi.org/10.1016/j.jfoodeng.2013.08.023

Peng, D., Yang, J., Li, J., Tang, C., & Li, B. (2017). Foams stabilized by β-lactoglobulin amyloid fibrils: Effect of pH. *Journal of Agricultural and Food Chemistry, 65*(48), 10658–10665. https://doi.org/10.1021/acs.jafc.7b03669

Sipe, J. D., Benson, M. D., Buxbaum, J. N., Ikeda, S., Saraiva, M. J. M., Westermark, P., et al. (2016). Amyloid fibril proteins and amyloidosis : Chemical identification and clinical classification international society of amyloidosis 2016 nomenclature guidelines amyloid fibril proteins and amyloidosis : Chemical identification and clinical classification I. *Amyloid: International Journal of Experimental & Clinical Investigation, 6129*. https://doi.org/10.1080/13506129.2016.1257986

Tang, C. H., & Sun, X. (2010). Physicochemical and structural properties of 8S and/or 11S globulins from mungbean [Vigna radiata (L.) Wilczek] with various polypeptide constituents. *Journal of Agricultural and Food Chemistry, 58*(10), 6395–6402. https://doi.org/10.1021/jf904254f

Thrane, M., Paulsen, P. V., Orcutt, M. W., & Krieger, T. M. (2017). *Soy protein: Impacts, production, and applications. Sustainable protein sources*. Elsevier Inc. https://doi.org/10.1016/B978-0-12-802778-3.00002-0

Wan, Y., & Guo, S. (2019). The Formation and disaggregation of soy protein isolate fibril: Effects of pH. *Food Biophysics, 14*(2), 164–172. https://doi.org/10.1007/s11483-019-09567-1

Wan, Z., Yang, X., & Sagis, L. M. C. (2016). Contribution of long fibrils and peptides to surface and foaming behavior of soy protein fibril system. *Langmuir, 32*(32), 8092–8101. https://doi.org/10.1021/acs.langmuir.6b01511

Willett, W., Rockström, J., Loken, B., Springmann, M., Lang, T., Vermeulen, S., et al. (2019). Food in the anthropocene: The EAT-lancet commission on healthy diets from sustainable food systems. *Lancet (London, England), 393*(10170), 447–492. https://doi.org/10.1016/S0140-6736(18)31788-4

Ye, X., Lendel, C., Langton, M., Olsson, R. T., & Hedenqvist, M. S. (2019). Protein nanofibrils: Preparation, properties, and possible applications in industrial nanomaterials. In *Industrial applications of nanomaterials*. Elsevier Inc. https://doi.org/10.1016/b978-0-12-815749-7.00002-5.